FEMS Yeast Research, 15, 2015, fou006

doi: 10.1093/femsyr/fou006
Research Article

RESEARCH ARTICLE

Role of cytoplasmic deadenylation and mRNA decay factors in yeast apoptosis

Kalidindi K. Raju[1,*], Sumathi Natarajan[2], N. Sunil Kumar[1], D. Anil Kumar[2] and Raghavendra NM[3]

[1]Department of Biotechnology, GRIET, Hyderabad 500090, Telangana, India, [2]Department of Biochemistry, Osmania University, Hyderabad 500007, Telangana, India and [3]Department of Medicinal Chemistry, Gokaraju Rangaraju College of Pharmacy, Hyderabad 500090, Telangana, India

*Corresponding author: Building 4; Department of Biotechnology, Gokaraju Ranagaraju Institute of Engineering and Technology, Bachupally, Kukatpally, Hyderabad 500090, Rangareddy district, Telangana, India. Tel: +919490928239;
E-mail: kalidindirj@gmail.com

One sentence summary: The Strong apoptotic phenotype observed in the double mutants of CCR4/PAN2 suggests role of ploy(A) tail length control in caspase-dependent apoptotic cell death in strains with defects in cytoplasmic deadenylation and Changes in transcript abundance of eIF4E and Pab1 in strains defective in deadenylation (ccr4Δ and), decapping (dcp2Δ and lsm1Δ strains) or cytoplasmic exosome function (ski2Δ) suggest decapping antagonists contribute to stress responses accompanying enhanced cell death.
Editor: Ian W. Dawes

ABSTRACT

Strains of *Saccharomyces cerevisiae* lacking factors involved in 5′ to 3′ mRNA decay pathway (*DCP1*, *DCP2*, *DHH1*, *PAT1*, *LSM1* and *LSM4*) exhibit caspase-dependent apoptosis and accelerated chronological aging. In the present study, yeast strains lacking mRNA decapping activation factors (*DCP2* and *LSM1*), cytoplasmic exosome function (*SKI2*) or cytoplasmic deadenylases (double deletion of *CCR4* and *PAN2*) showed typical markers of eukaryotic apoptosis such as increased cellular reactive oxygen species levels, externalization of phosphatidyl serine, chromatin fragmentation, enhanced caspase gene (*YCA1*) expression and protein activity in mid-log phase cultures. The transcript levels of negative regulators of mRNA decapping (eIF4E and Pab1) were considerably elevated in strains defective in cytoplasmic deadenylation and reduced in strains lacking cytoplasmic 3′ to 5′ exosome function or decapping activators. Among the yeast strains studied, *lsm1*Δ and *ccr4*Δ*pan2*Δ mutants displayed strongest apoptotic phenotype followed by mutants lacking *DCP2* or *SKI2*. Among yeast strains exhibiting deadenylation defects, slight apoptotic phenotype was observed in *ccr4*Δ mutants and cell death markers imperceptible in *pan2*Δ mutants.

Key words: deadenylases; mRNA degradation; apoptosis; metacaspase; decapping; exosome; real time-PCR; flow-cytometer; fluorescent microscopy; yeast

INTRODUCTION

In eukaryotes, programmed cell death (PCD) is a genetically regulated self-destruction process for the elimination of damaged or unwanted cells. It plays an important role in the development and maintenance of the integrity of organisms. The basic molecular machinery governing apoptosis in mammals has been very much conserved in yeast, including the yeast metacaspase Yca1p, the mitochondrially located proteins such as apoptosis-inducing factor 1 (Aif1p), HtrA2/Omi (Nma111p) and AMID (Ndi1p), and the anti-apoptotic proteins Cdc48p and Bir1p (Fahrenkrog, Sauder and Aebi 2004; Wissing *et al.*, 2004; Mazzoni *et al.*, 2003b, 2005; Walter *et al.*, 2006; Braun and Zischka 2008; Mazzoni and Falcone 2008; Carmona-Gutierrez and Madeo 2009). Apoptosis in yeast may be initiated during physiological

Received: 29 May 2014; **Accepted:** 25 November 2014

scenarios such as ageing and failed mating, or exposure to external stimuli such as low doses of H_2O_2 or acetic acid. Various morphological and biochemical events observed in apoptotic cells are chromatin fragmentation and its condensation (margination), externalization of phosphatidylserine to the outer leaflet of the plasma membrane, mitochondrial fragmentation, cytochrome *c* release, cytoskeletal perturbations and histone H2B phosphorylation (Ludovico *et al.*, 2002; Ahn *et al.*, 2006; Carmona-Gutierrez and Madeo 2009; Carmona-Gutierrez *et al.*, 2010). Similar to mammalian PCD, ROS act as central regulators of yeast apoptosis (Madeo *et al.*, 1999).

The messenger RNA decay pathways and decay factors are well conserved in all eukaryotes from yeast to humans. Two major pathways of mRNA decay exist in eukaryotes. Both pathways are initiated by poly(A) shortening of the mRNA. In the 5′ to 3′ decay pathway, the Dcp1p/Dcp2p decapping enzyme complex can hydrolyze the cap structure following deadenylation by Pan2p and Ccr4p enzymes and the mRNA is subsequently degraded from the 5′ end by Xrn1 nuclease (Muhlrad, Decker and Parker 1994; Brown and Sachs 1998; Dunckley and Parker 1999; Stevens 2001; Tucker *et al.*, 2001; Van Dijk *et al.*, 2002; Steiger *et al.*, 2003; Parker and Song 2004; Franks and Lykke-Andersen 2008). In the 3′ to 5′ decay pathway, deadenylated mRNAs are degraded in a 3′ to 5′ exonucleolytic manner and require two multiprotein complexes: the exosome containing various 3′-exonucleases and the Ski complex consisting of RNA helicase Ski2p, Ski3p, Ski7p and Ski8p (Anderson and Parker 1998; Van Hoof *et al.*, 2000: Araki *et al.*, 2001). In the 5′ to 3′ pathway, the heterooctameric Lsm1p-7p-Pat1p complex (made of seven Sm-like proteins, Lsm1p through Lsm7p and Pat1p) interacts with several decay factors and activates decapping *in vivo* (Bouveret *et al.*, 2000; Tharun *et al.*, 2000; Tharun and Parker 2001). Poly A binding protein (Pab1p) when bound to the 3′ poly(A) tail promotes interaction of eukaryotic translation initiation factor (eIF4E) to the 5′cap of mRNA and protect the 5′ end from decapping (Tarun and Sachs 1996; Coller, Gray and Wickens 1998; Wells *et al.*, 1998; Schwartz and Parker 1999; Amrani *et al.*, 2008).

Misregulation of apoptosis or mRNA turnover can result in many human diseases (Steller 1995; Streicher *et al.*, 2007). Apoptotic studies in yeast suggested interconnecting mechanism between mRNA metabolism and apoptosis (Mazzoni *et al.*, 2003b, 2005). Expression of a truncated form of Kluyveromyces lactis LSM4 (Kllsm4Δ1, Mazzoni and Falcone 2001 and Mazzoni *et al.*, 2003a) in a *Saccharomyces cerevisiae* strain where the only copy of the essential gene LSM4, a component of a complex promoting pre-messenger RNA splicing and mRNA decapping, is expressed from a GAL promoter, leads to increased mRNA stability and caspase-mediated-apoptotic death in glucose medium (Cooper, Johnston and Beggs 1995; Tharun *et al.*, 2000; Mazzoni *et al.*, 2003b). The disruption of *YCA1* in the *Kllsm4Δ1* mutant background rescued cells from apoptotic death without affecting mRNA stability (Mazzoni *et al.*, 2005). Genomic expression analysis showed that strains lacking genes encoding proteins which function in RNA metabolism were oversensitive to oxidative stress (Gasch *et al.*, 2000; Thorpe *et al.*, 2004). These included genes encoding rRNA helicases (*DBP3*, *DBP7*), rRNA processing factors (*NOP12*, *NSR1*), mRNA deadenylases (*CCR4*, *POP2*) and several mitochondrial RNA splicing components (Higgins *et al.*, 2002; Thorpe *et al.*, 2004). Moreover processing bodies (P-bodies), specific cytoplasmic foci for mRNAs decapping and decay, may play important roles during cellular responses to stress in that their size and number increased in several stress conditions such as oxidative stress, glucose deprivation, osmotic stress, ultraviolet light and late stage of growth (D'AddarioFalconeSheth and Parker 2003; Teixeira *et al.*, 2005; Mazzoni, D'Addario and Falcone 2007).

In the present study, apart from yeast strains lacking factors for 5′ to 3′ mRNA decapping and decay (*DCP2* and *LSM1*), mutants defective in 3′ to 5′ cytoplasmic exosome function (*SKI2*) or deadenylation (double deletion of *CCR4* and *PAN2*) were screened for various biochemical and morphological features of apoptosis in the mid-log phase cultures. Since eIF4E and Pab1p are known to promote mRNA stability by antagonizing decapping, mRNA levels of decapping inhibitors were quantitated to have any role in cell death (Coller *et al.*, 1998; Schwartz and Parker 1999, 2000).

MATERIALS AND METHODS

Strains and growth conditions

Cells were grown in a mechanical shaker (220 rpm) at 26°C in minimal medium (0.5% ammonium sulphate, 0.17% yeast nitrogen base) containing 2% glucose (SD) supplemented with 0.079% Synthetic *Complete* drop-out Medium *Mix*. Yeast strains used in this study are listed in Table 1.

Yeast strains were harvested at mid-log phase OD $\leq$ 0.5 for quantitative RT-PCR (qRT-PCR), flow cytometry and microscopic examination studies. For cell viability studies, inoculation was carried out by addition of a freshly revived colony of *S. cerevisiae* to the medium and was incubated under shaking conditions for 15 days on a rotary shaker (220 rpm) at ambient temperature (26 $\pm$ 2°C). Aliquots of the culture broth were withdrawn at different time points, serially diluted using sterile saline (0.85%) and transferred to YPD agar (1% yeast extract, 2% peptone, 2% dextrose and 2% agar) using a spread plate technique. Plates were incubated at 26 $\pm$ 2°C for 3 days. Viable cell counts were obtained at the end of the incubation period by counting colonies.

Assessment of intracellular reactive oxygen species (ROS) by flow cytometry

Free intracellular ROS were detected with dihydrorhodamine 123 (DHR123) (Molecular Probes, Eugene, OR, USA). Multiple ROS convert DHR123 to the stable fluorescent derivative DHR with excitation and emission wavelengths at 500 and 530 nm, respectively. DHR123 was added from a 1 mg ml^{-1} stock solution in ethanol to 5 $\times$ 10^6 cells ml^{-1} suspended in PBS, reaching a final concentration of 10 μg ml^{-1}. Cells were viewed without further processing through a rhodamine optical filter after 90 min incubation at 28°C in the dark as described previously (Madeo *et al.*, 1999). For flow cytometric analysis, the samples were labelled with DHR123 as described above except that 1 $\times$ 10^6 cells were washed with PBS prior to acquisition on a Guava easyCyte 8HT flow cytometer (Millipore). 488 excitation laser and 525/30 nm bandpass filters were used to capture the emission of rodamine. For all the assays done, data were acquired with Express Pro software and analysed by FlowJo software (Version 7.6). 20 000 events were acquired at a flow rate of 0.59 μL s^{-1} per sample.

Annexin V-FITC/PI staining

Exposed phosphatidylserine was detected by reaction with FITC-coupled annexin V as described previously (Madeo, Frohlich and Frohlich 1997). Yeast cells were washed in sorbitol buffer (1.2 M

Table 1. Yeast strains used in this study.

Strain no.	Genotype
yRP840	*MAT a, leu2, his4, trp1, ura3, cup1LEU2PM*
yRP1365	*MAT α; leu2; trp1; lys2; ura3; cup1Δ::LEU2PM; lsm1Δ::TRP1*
yST456	*MatA, his4, leu2, trp1, ura3, lys2, cup1Δ::LEU2PM, dcp2Δ::TRP1*
yRP1195	*MAT a, his4, leu2, trp1, ura3, cup1::LEU2PM, ski2::LEU2*
yRP1616	*MAT a, trp1, ura3, leu2, his4, cup1::LEU2PM, ccr4Δ::NEO*
yRP1619	*MAT a, ura3, leu2, his4, cup1::LEU2PM, pan2Δ::URA3*
yRP1620	*MAT a, trp1, ura3, leu2, his4, cup1::LEU2PM, ccr4Δ::NEO, pan2Δ::URA3*

Table 2. Primers used for qRT-PCR.

oligo	Sequence
YCA1 Forward	5′ CATATGCCACAGGAAACAGG 3′
YCA1 Reverse	5′ CACGCGTTCTCTATCCACAT 3′
Pab1 Forward	5′ GTTGCCATTGCTCAAAGAAA 3′
Pab1 Reverse	5′ CATTGGAGGCATGAATTGAC 3′
eIF4E Forward	5′ CCGTCGATAAATCTGAGTCG 3′
eIF4E Reverse	5′ ATGGTAGTTCGTGTGGCTCA 3′
SCR1 Forward	5′ GGCTGTAATGGCTTTCTGGT 3′
SCR1 Reverse	5′ ACGGTGCGGAATAGAGAACT 3′

sorbitol, 0.5 mM $MgCl_2$, 35 mM potassium phosphate, pH 6.8), cell wall digested with 20 U ml^{-1} lyticase (Sigma Chemical Co.) in sorbitol buffer for 2 h at 28°C, harvested, washed in binding buffer (10 mM Hepes/NaOH, pH 7.4, 140 mM NaCl, 2.5 mM $CaCl_2$) containing 1.2 M sorbitol buffer and resuspended in binding buffer/sorbitol. 10 μl annexin-FITC (AnnexinV Apoptosis Detection Kit; Invitrogen) was added to 190 μl cell suspension, and then incubated for 15 min at room temperature. The cells were harvested, resuspended in 190 μl binding buffer/sorbitol and incubated in 10 μl propidium iodide (PI) for 5 min prior to acquisition on a flow cytometer. 488 excitation laser, 525/30 and 690/50 nm bandpass filters were the parameters used for fluorescence acquisition from annexin V FITC and PI, respectively.

Terminal deoxynucleotidyl transferase-mediated dUTP nick end labelling (TUNEL) staining

DNA strand breaks were monitored by TUNEL with the In Situ Cell Death Detection kit, Fluorescein (Roche Applied Science). TUNEL labels free 3′-OH termini with fluorescein isothiocyanate (FITC)-labelled deoxyuridine triphosphate (dUTP), which can be detected under epifluorescence microscope as described previously (Madeo *et al.*, 1997). Yeast cells were fixed with 3.7% (vol/vol) formaldehyde for 1 h. Cell wall was digested with 20 U ml^{-1} lyticase (Sigma-Aldrich, St. Louis, MO) for 2 h at 28°C. Spheroplasts were then applied to polylysine-coated slides and rinsed with phosphate-buffered saline (PBS), incubated in permeabilization solution (0.1%, vol/vol, Triton X-100 and 0.1%, wt/vol, sodium citrate) for 2 min on ice, rinsed twice with PBS and incubated with 15 μl of TUNEL reaction mixture (200 U ml^{-1} terminal deoxynucleotidyl transferase, 10 mM FITC-labelled dUTP, 25 mM Tris-HCl, 200 mM sodium cacodylate and 5 mM cobalt chloride) for 60 min at 37°C. Finally, the slides were rinsed three times with PBS, and a coverslip was mounted. Microscope and image acquisitions were performed in epifluorescence microscope (Lawrence and Mayo; Model No. LM-52–3000) at 40× objective.

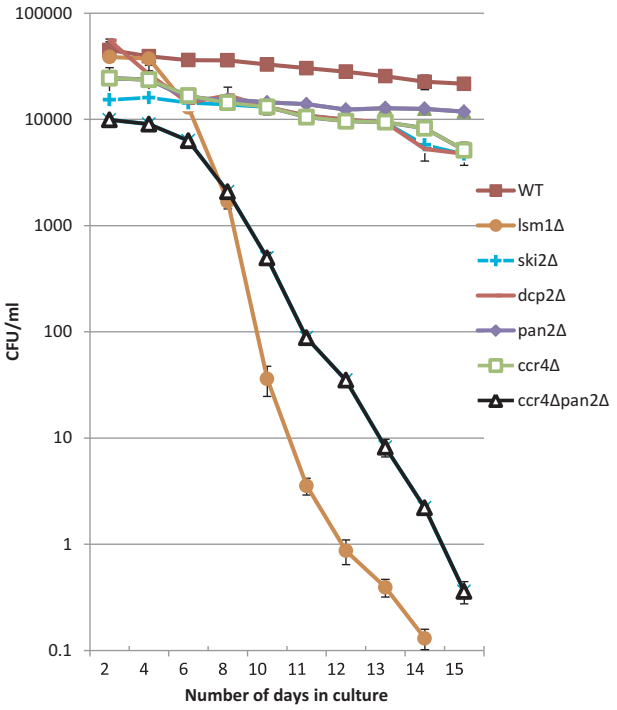

Figure 1. *Viability of different yeast strains measured during stationary phase.* Viable cell counts (colony forming units/ml) collected at different time points (2, 4, 6, 8, 10, 11, 12, 13, 14 and 15 days in culture) and plated on yeast extract peptone dextrose (YPD) agar [WT (yRP840), *lsm1Δ* (yRP1365), *dcp2Δ* (yST456), *ski2Δ* (yST394), *ccr4Δ* (yRP1616), *pan2Δ* (yRP1619) and *ccr4Δpan2Δ* (yRP1620)]. Each time point on the graph represents mean value from three independent determinants ($n = 3$). Error bars represent standard deviation.

DAPI staining

For nuclear morphology, cells in the mid-log phase were fixed with 70% (v/v) ice cold ethanol and stained with DAPI 0.1 μg ml^{-1} (Sigma Aldrich) for 15 min in dark. The cells were then washed twice with PBS, resuspended in 100 μl of PBS and mounted on slides using CC mount (Sigma Aldrich). The imaging was carried out with 63X objective of confocal microscope (Leica TCS SP5-II) at an emission wavelength of 416–522 nm and excitation laser 405 nm diode.

In vivo caspase detection by flow cytometric analysis

Endogenous caspase activity was measured using Calbiochem® Caspase Detection Kit. The assay utilizes a cell permeable and irreversible caspase inhibitor (VAD-FMK) conjugated to FITC as the fluorescent *in vivo* marker. Yeast cells were harvested at

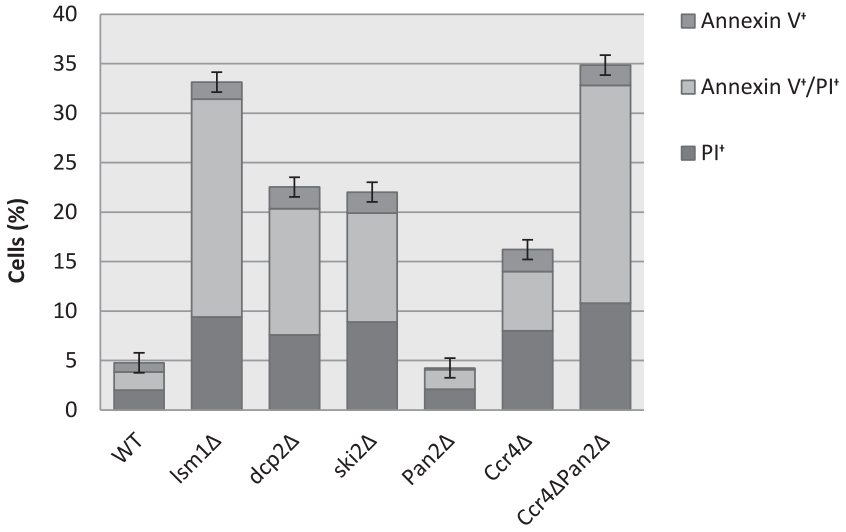

Figure 2. Annexin V-FITC/PI apoptosis assay on different yeast strains. Yeast strains harvested at mid-log phase OD ≤ 0.5 (WT, *lsm1Δ*, *dcp2Δ*, *ski2Δ*, *ccr4Δ*, *pan2Δ and ccr4Δpan2Δ* mutants) were stained with Annexin V-FITC/PI and acquired by flow cytometer. Graph represents AnnexinV, PI and Annexin V/PI cell percentage (%). Each bar represents mean of triplicate samples ($n = 3$). Error bars indicate standard deviations.

mid-log phase (OD ≤ 0.5), washed once with PBS and incubated with 1 μl FITC-VAD-FMK at 35°C for 45 min. After completion of staining, cells were washed twice with wash buffer and the activated caspases quantified by flow cytometry using FL-1 channel. Data acquisition and software analysis were performed similar to ROS assay described above.

RNA preparations

Total RNA was isolated from exponential phase cells (OD ≤ 0.5) using the High Pure RNA Isolation Kit (Roche, Germany) as described by the manufacturer. A total of 10 μg total RNA was treated with 2 U Turbo DNase I (Life Technologies) for 30 min at 37°C to eliminate genomic DNA (gDNA) contamination. RNA integrity was analysed by electrophoresis in 1% agarose gels in 1× TBE (89 mM Tris borate, 2 mM EDTA [pH 8.3]), stained with ethidium bromide and visualized under UV light. Nucleic acid was quantified by measuring the absorbance at 260 nm using nanodrop technology. First-strand cDNA synthesis was performed using Maxima First Strand cDNA Synthesis Kit (Thermo Scientific). The reverse transcription reaction contained 1 μg of treated RNA, Maxima Enzyme Mix (Maxima Reverse Transcriptase and RiboLock RNase Inhibitor) and 5X Reaction Mix (reaction buffer, dNTPs, oligo $(dT)_{18}$ and random hexamer primers) in a 20 μl final volume. The mixture was incubated at 50°C for 30 min. After first-strand synthesis, reactions were heat-inactivated at 85°C for 5 min.

Real-time PCR

The expression level of Pab1, elf4E and Yca1 mRNAs was determined using qRT-PCR. The primers used to amplify the selected genes were designed using GenScript real-time PCR (TaqMan) primer design software. Reactions were set up in a total volume of 25 μl using 2 μl of template cDNA, 12.5 μl MESAGREEN qPCR Mastermix Plus for SYBR Green Assay (Eurogenetic) and 0.6 μM each of gene-specific primers, quantitation performed in the ABI 7500 real time PCR system (Applied Biosystems). The reaction conditions were 95°C for 15 s; 40 cycles of 95°C for 1 min, 50°C for 1 min and 72°C for 35 s with a single fluorescence measurement. Specificity of the PCR products was confirmed by analysis of the dissociation curve (1 cycle of 95°C for 15 s, 60°C for 1 min and 95°C for 15 s). Additionally, the amplicons' expected size and the absence of non-specific products were confirmed by analysis of the real-time PCR products in 1% agarose gels in 1× TBE, stained with ethidium bromide and visualized under UV light. Comparative Ct method or 2^(−ΔΔCt) was followed to calculate the fold change in gene expression normalized to an unaffected reference gene, the SCR1 RNA and relative to the wild-type (WT) control (yRP 840). Primers are described in Table 2.

RESULTS

Survival of different yeast strains in growth media

Viable cell counts in stationary-phase cultures of different yeast strains incubated on a rotary shaker for 15 days post-inoculation are shown in Fig. 1. In *lsm1Δ* mutant strains, cell count diminished from 7 $\log_{10}$ CFU ml^{-1} at the onset of the stationary phase (2 days post-inoculation) to almost 0 at the end of incubation (13th day from the onset of stationary phase). In the *ccr4Δpan2Δ* mutant strains, cell count diminished from 7 $\log_{10}$ CFU ml^{-1} at the onset of the stationary phase to 2 $\log_{10}$ CFU ml^{-1} on the 13th day from the onset of stationary phase. In *ski2Δ*, *dcp2Δ* and *ccr4Δ* strains, the cell count slightly reduced from 7 $\log_{10}$ CFU ml^{-1} at the onset of the stationary phase (2 days post-inoculation) to 6 $\log_{10}$ CFU ml^{-1} at the end of incubation (13th day from the onset of stationary phase). On the other hand, the viable cell numbers in WT and *pan2Δ* strains remained stable (∼7 $\log_{10}$ CFU ml^{-1}) both at the beginning and at the end of the incubation in stationary phase (Fig. 1).

Apoptosis in strains defective in decapping, cytoplasmic exosome function or deadenylation requires YCA1

Plasmamembrane translocation of phosphatidylserine from the inner to the outer membrane leaflet is one of the early markers of apoptosis. The percentage of apoptosis in WT as well as mutants defective in decapping (i.e. *dcp2Δ* and *lsm1Δ*), cytoplasmic exosome function (*ski2Δ*) or deadenylation (*pan2Δ*,

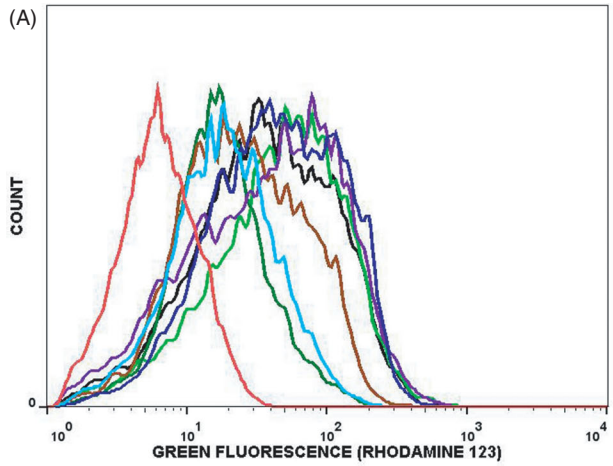

	Sample Name	Median : GRN-HLog	Geometric Mean : GRN-HLog
	UNSTAINED.FCS	6.28	6.26
	yRP840.FCS	18.5	18.2
	lsm1Δ.FCS	45.1	43.1
	ski 2Δ.FCS	42.3	35.9
	ccr4Δ.FCS	24.5	25.0
	pan2 Δ.FCS	16.9	17.4
	ccr4Δ pan2Δ.FCS	50.2	43.9
	dcp2Δ.FCS	37.2	35.5

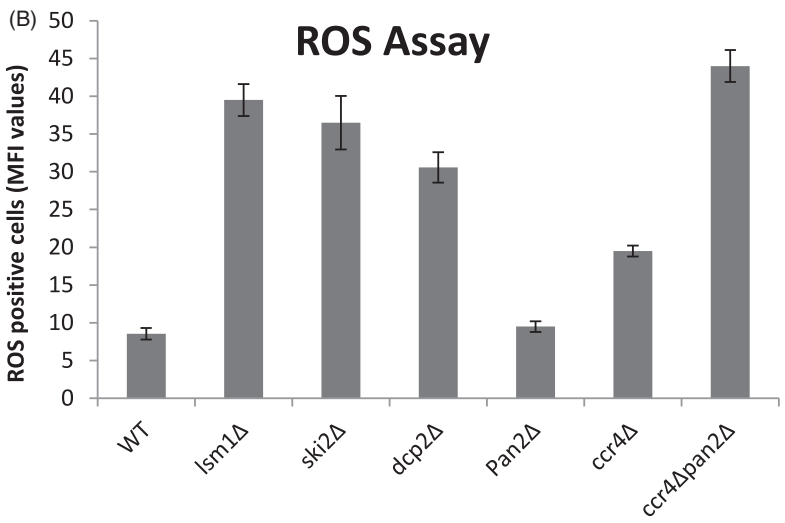

Figure 3. (A) Representative graph showing cellular ROS levels in different yeast strains. Cells were incubated with dihydrorhodamine 123 (DHR123), and ROS levels were analysed by flow cytometer. The table in the right represents MFI values for ROS against each individual strain (WT, *lsm1Δ*, *dcp2Δ*, *ski2Δ*, *ccr4Δ*, *pan2Δ and ccr4Δpan2Δ* mutants). **(B)** Bar graph shows ROS generation in different yeast strains. Cells were incubated with DHR123 and ROS levels were studied by flow cytometry. The different yeast strains used for the study are represented on X-axis. Bar graph shows results from the mean of three independent experiments and relative DHR fluorescence was expressed as MFI values.

ccr4Δ and *ccr4Δpan2Δ*) were assessed by Annexin V-FITC/PI staining. Annexin V binds to phosphatidylserine with high affinity in the presence of $Ca2^{+}$, this combined with the membrane-impermeable dye PI, gives a picture of early and late apoptotic cells. In strains with deletion of *LSM1* and double deletion of *CCR4/PAN2* ~24% of cells are Annexin V/PI positive, whereas ~13% of *ski2Δ*, ~15% of *dcp2Δ* cells and 9% of *ccr4Δ* cells are Annexin V/PI positive. In WT and *pan2Δ* cells, basal level of apoptosis was observed as less than 2% of cells show positive staining (Fig. 2).

Another key event in apoptotic cells is generation of ROS. Previously reported that about 40% of *Kllsm4Δ1* cells displayed intense intracellular staining with dihydrorhodamine 123 (Mazzoni *et al.*, 2003b). Flow cytometric studies were carried to determine cellular ROS levels by incubation with DHR123. Increased cellular ROS levels were observed in the mutants defective in decapping (*dcp2Δ* and *lsm1Δ* strains), cytoplasmic exosome function (*ski2Δ*) or double mutant defective in deadenylation (*ccr4Δpan2Δ* mutants). Intense cellular fluorescence was observed in *ccr4Δpan2Δ* and *lsm1Δ* cells with 44 ± 2.12 and 39.5 ± 2.13 median fluorescence intensity (MFI) respectively, whereas *ski2Δ*, *dcp2Δ* and *ccr4Δ* cells show 36 ± 3.53, 30.57 ± 2.01 and 18.5 ± 0.70 MFI values respectively with DHR123 staining (Fig. 3a and b). Basal levels of ROS levels were observed in WT and *pan2Δ* strains with less than 10 MFI (Fig. 3a and b).

Another hallmark of apoptosis in yeast is DNA breakage with generation of free 3′-OH group that can be detected by the TUNEL assay (Madeo *et al.*, 1999, 2002). Nearly 40% of cells in *lsm1Δ* strain and 45% of cells in *ccr4Δpan2Δ* strain showed intense green fluorescent nuclei indicating DNA fragmentation in large number of cells. In *dcp2Δ* or *ski2Δ* mutants ~25% of cells and in *ccr4Δ* mutants ~19% of cells show green fluorescence. In WT and *pan2Δ* strains, <6% of cells exhibit DNA strand breakage (Fig. 4a and b).

WT as well as mutants defective in decapping (i.e. *dcp2Δ* and *lsm1Δ*), cytoplasmic exosome function (*ski2Δ*) or deadenylation (*pan2Δ*, *ccr4Δ* and *ccr4Δpan2Δ*) were analysed for nuclear fragmentation by 4, 6-diamidino-2-phenylindole (DAPI) staining. WT and *pan2Δ* mutant cells had a normal nuclear morphology as evidenced by single round spot, whereas in the mutants defective in decapping (i.e. *dcp2Δ* and *lsm1Δ*), cytoplasmic exosome function (*ski2Δ*) or double mutant defective in

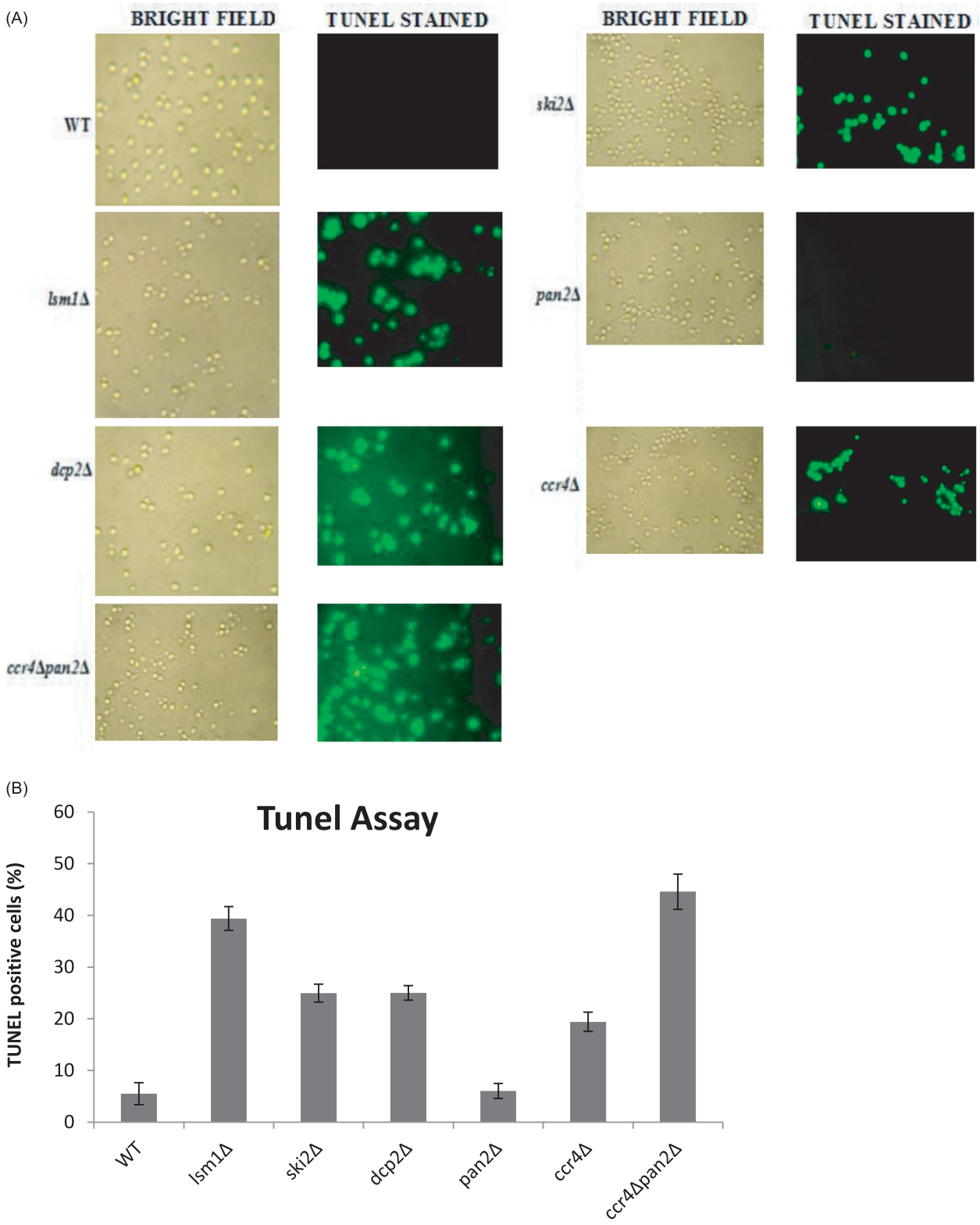

Figure 4. (A) Epifluorescent microscopy assessment of DNA strand breaks. Different yeast strains (WT, *lsm1Δ*, *dcp2Δ*, *ski2Δ*, *ccr4Δ*, *pan2Δ and ccr4Δpan2Δ* mutants) harvested at mid-log phase OD ≤ 0.5 were assessed for DNA strand breaks (green fluorescent cells in TUNEL assay shown in right column). Left column: bright-field pictures, Right column: TUNEL stained cells. **(B)** Graphical representation of percentage (%) of cells undergoing apoptosis as analysed by epifluorescent microscopy. TUNEL was performed in different yeast strains harvested at mid-log phase OD ≤ 0.5 (WT, *lsm1Δ*, *dcp2Δ*, *ski2Δ*, *ccr4Δ*, *pan2Δ and ccr4Δpan2Δ* mutants). 150–200 cells/glass slide were counted each time, and each bar represents mean of triplicate samples ($n = 3$). Error bars indicate standard deviation.

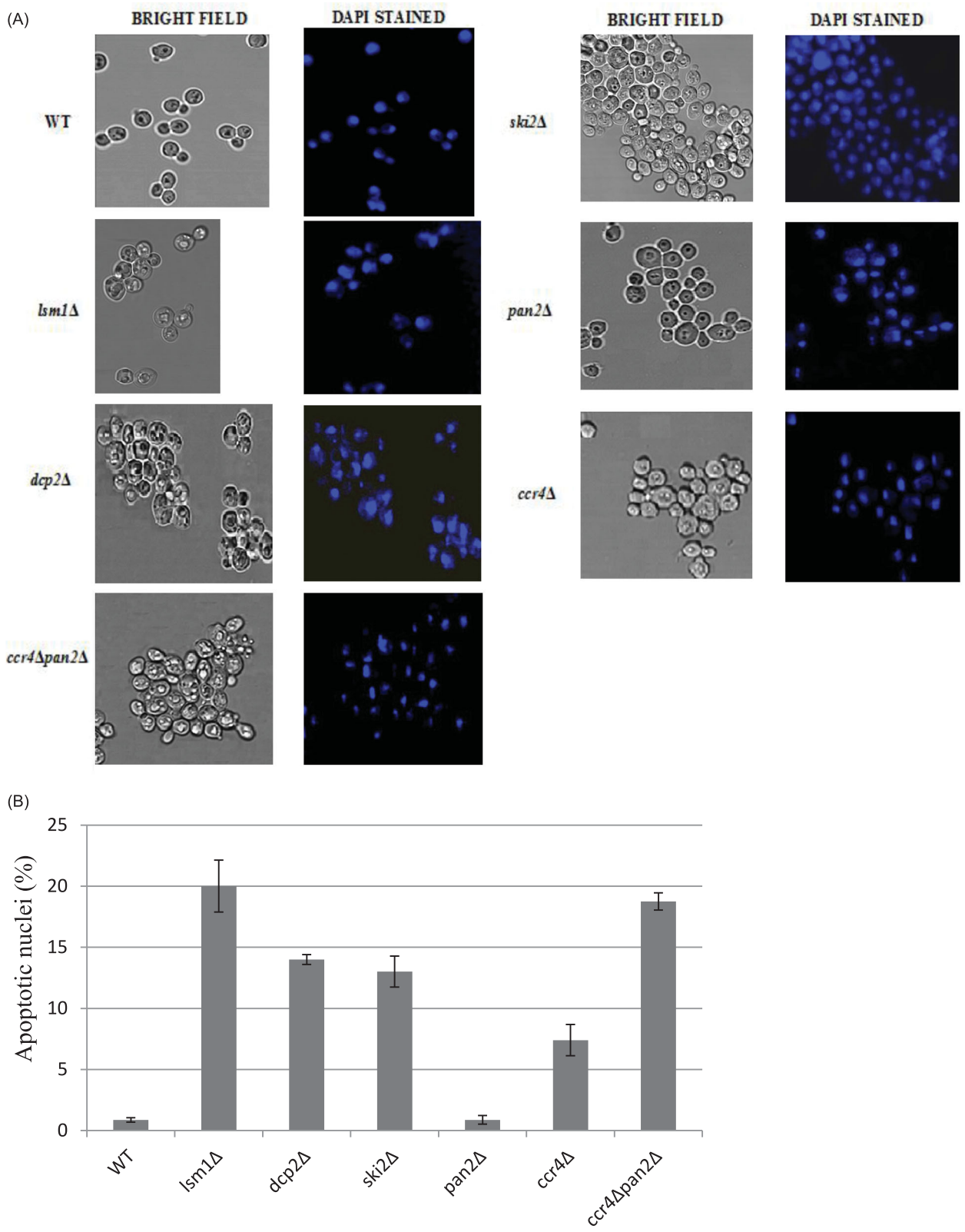

Figure 5. (A) Confocal microscopy images of different yeast strains following DAPI staining. WT, *lsm1*Δ, *dcp2*Δ, *ski2*Δ, *pan2*Δ, *ccr4*Δ and *ccr4*Δ*pan2*Δ cells were analysed for nuclear fragmentation (blue fluorescent cells in DAPI test) by staining with DAPI. Cells were imaged with a confocal microscope. Left column: phase contrast, Right column: DAPI stained cells. **(B)** Graphical representation of percentage (%) of apoptotic nuclei in different yeast strains as analysed by confocal microscopy. DAPI assay was performed in different yeast strains harvested at mid-log phase OD $\leq$ 0.5. 50–75 cells/slide were counted each time, and each bar represents mean of triplicate samples ($n = 3$). Error bars indicate standard deviation. Nearly 20% of *lsm1*Δ cells and 19% of *ccr4*Δ*pan2*Δ cells displayed apoptotic nuclei, followed by dcp2Δ (~14%), *ski2*Δ (~13%) and *ccr4*Δ cells (~18%). Less than 1% of WT and *pan2*Δ cells exhibited nuclear fragmentation.

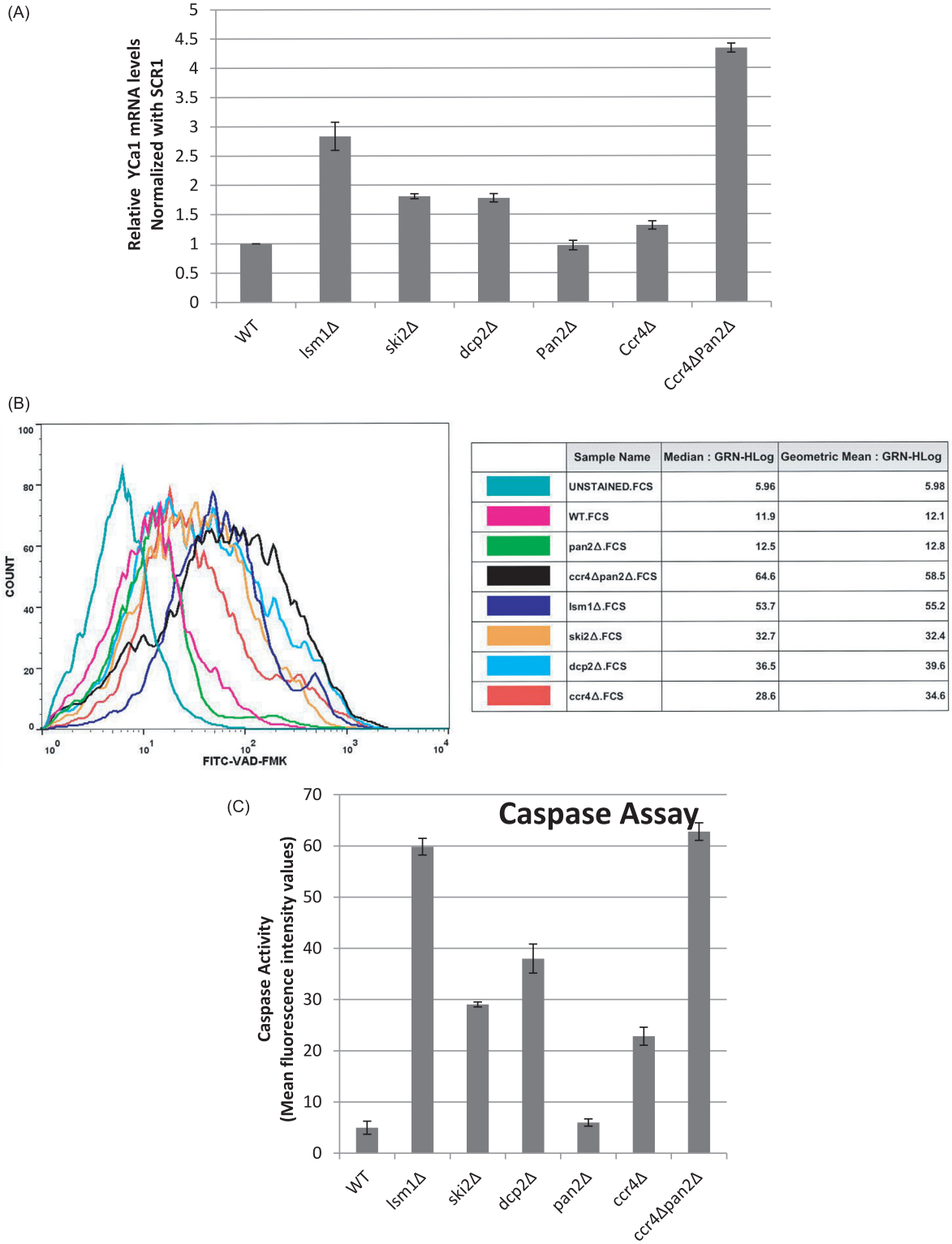

Figure 6. (A) Quantification of caspase mRNAs isolated from different yeast strains at mid-log phase (OD ≤ 0.5) (WT, *lsm1Δ*, *dcp2Δ*, *ski2Δ*, *ccr4Δ*, *pan2Δ and ccr4Δpan2Δ* mutants). Each qRT-PCR experiment was performed thrice in duplicate. C_T values for caspase gene (YCA1) and standard reference (SCR1) are average of results from one typical experiment. The C_T values of both the WT and mutant strains were normalized to standard reference gene SCR1. Data and error bars represent the average and standard deviation of two independent experiments ($n = 4$). **(B)** Representative graph showing *in vivo* caspase activity in different yeast strains (i.e. untreated WT, WT, *lsm1Δ*, *dcp2Δ*, *ski2Δ*, *ccr4Δ*, *pan2Δ* and *ccr4Δpan2Δ* mutants). Cells were incubated with FITC-labelled caspase inhibitor (VAD-FMK) and caspase activation was analysed by flow cytometer. The table in the right represents MFI values of the activated caspases contained in each individual strain (WT, *lsm1Δ*, *dcp2Δ*, *ski2Δ*, *ccr4Δ*, *pan2Δ and ccr4Δpan2Δ* mutants). **(C)** Bar graph representing caspase activity (expressed as MFI values) contained in different yeast strains labeled on X-axis. 10 000 events were acquired each time at a flow rate of 0.59 μL s^{-1} per sample. Data and error bars represent the average and standard deviation of three independent experiments ($n = 3$).

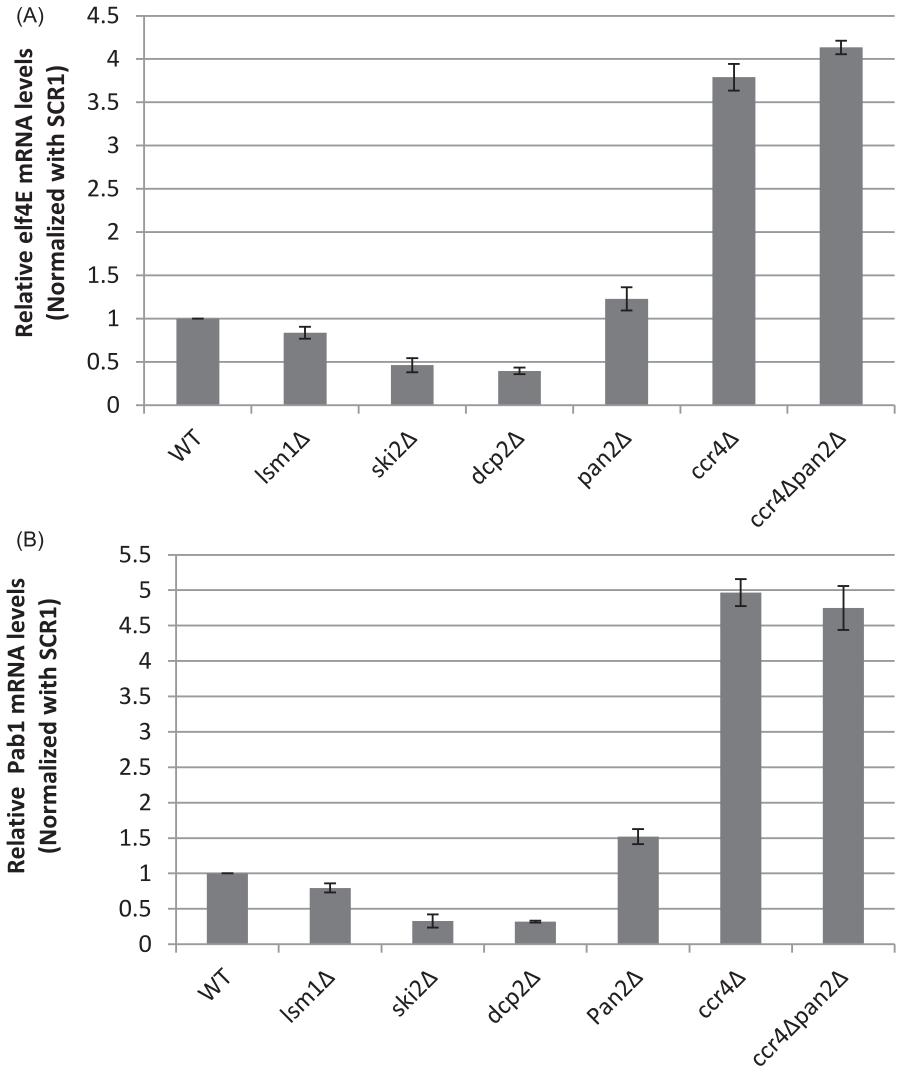

Figure 7. (A) and **(B)** represent relative eIF4E and Pab1 transcript levels respectively in different yeast strains (WT, *lsm1Δ*, *dcp2Δ*, *ski2Δ*, *ccr4Δ*, *pan2Δ and ccr4Δpan2Δ* mutants). Each qRT-PCR experiment was performed four times in duplicate. C_T values for each gene (*eIF4E*, *PAB1* and standard reference gene (*SCR1*) are averages of results from one typical experiment. Data and error bars represent the average and standard deviation of two independent experiments ($n = 4$).

deadenylation (*ccr4Δpan2Δ*), nuclei appeared fragmented and DNA condensed. In *ccr4Δ* mutants, minor defects in nuclear morphology and chromatin appearance were observed (Fig. 5a and b).

Yeast metacaspase (*YCA1*) plays an important role in regulating apoptosis triggered by oxidative stress, chronological ageing or stabilization of mRNAs (Madeo *et al.*, 2002;Herker *et al.*, 2004). qRT-PCR was performed to analyse *YCA1* transcript levels in WT as well as mutants defective in decapping (*dcp2Δ* and *lsm1Δ* strains), cytoplasmic exosome function (*ski2Δ*) or deadenylation (*pan2Δ*, *ccr4Δ* and *ccr4Δpan2Δ* strains). Except *pan2Δ* strain, *dcp2Δ*, *ski2Δ*, *lsm1Δ*, *ccr4Δ* and *ccr4Δpan2Δ* mutants showed increased *YCA1* transcript levels relative to WT strain. In *lsm1Δ* and *ccr4Δpan2Δ* mutants, *YCA1* mRNA levels were elevated 3- and 4-fold, respectively. In *pan2Δ* mutant cells, *YCA1* mRNA levels were similar to the WT (Fig. 6a). In addition to *YCA1* expression studies, caspase protein activation *in vivo* was quantitated with FITC-labelled VAD-FMK by flow cytometry in strains defective in deadenylation and mRNA decay. Based on MFI values relative to untreated WT control, *lsm1Δ* and *ccr4Δpan2Δ* mutants display highest caspase activity with 59.85 ± 1.63 and 62.8 ± 1.69 MFI respectively followed by *dcp2Δ* (38.25 ± 2.82 MFI), *ski2Δ* (29.05 ± 0.49 MFI) and *ccr4Δ* (22.85 ± 1.76 MFI). Non-apoptotic WT and *pan2Δ* strains showed basal levels of caspase activity with less than six MFI (Fig. 6b and c).

Altered transcript abundance of decapping antagonists in the mutant strains

qRT-PCR was performed to analyse the Pab1 and elf4E transcript levels in strains exhibiting apoptosis. Strains exhibiting deadenylation defects (*ccr4Δ* and *ccr4Δpan2Δ* mutants) accumulate nearly 4-fold higher eIF4E and 5-fold higher Pab1 mRNA levels relative to WT. Pab1 and eIF4E transcript levels were considerably reduced in *dcp2Δ*, *lsm1Δ* and *ski2Δ* mutants relative to WT. In *pan2Δ* strains, Pab1 and eIF4E mRNA levels were slightly elevated than WT (Fig. 7a and b).

DISCUSSION

mRNA decay defects in yeast mutants defective in decapping (*lsm1Δ*, *lsm4Δ* or *dcp2Δ* strains) trigger caspase-dependent apop-

tosis (Mazzoni *et al.* 2003b, 2005). qRT-PCR, flow cytometry and microscopic studies suggest caspase-dependent apoptotic cell death in strains defective in cytoplasmic exosome function (*ski2*Δ mutants) or deadenylation (*ccr4*Δ and *ccr4*Δ*pan2*Δ mutant). The characteristic feature of strains screened for apoptotic markers (i.e. *dcp2*Δ, *lsm1*Δ *ski2*Δ, *ccr4*Δ or double mutant *ccr4*Δ*pan2*Δ) is clear-cut stabilization of multiple mRNAs (Decker and Parker 1993; Bouveret *et al.*, 2000; Tharun *et al.*, 2000; Tucker *et al.*, 2001; Mazzoni *et al.*, 2005; Meaux and Van Hoof 2006; Funakoshi *et al.*, 2007; Yoon, Choi and Parker 2010). Ccr4p is the predominant deadenylase subunit in yeast and *ccr4* mutants are known to exhibit accumulation of all mRNAs tested with 3′ poly(A) tails of an intermediate length (∼25–45 adenosines) (Tucker *et al.*, 2001; Beilharz and Preiss 2007). Double mutants of *CCR4/PAN2* were reported to be deficient in cytoplasmic deadenylation and accumulate all mRNAs tested thus far with longer poly(A) tails (>55 adenosines) suggesting longer poly(A) tail length of the accumulated mRNAs contribute to enhanced cell death in *ccr4*Δ*pan2*Δ strain than *ccr4*Δ strain (Tucker *et al.*, 2001; Beilharz and Preiss 2007). Similar to WT strain, *pan2*Δ mutants do not exhibit cytoplasmic deadenylation defects as well as characteristic features of metazoan apoptosis (Tucker *et al.*, 2001). Changes in transcript abundance of eIF4E and Pab1 in strains defective in deadenylation (*ccr4*Δ and *ccr4*Δ*pan2*Δ mutants), decapping (*dcp2*Δ and *lsm1*Δ strains) or cytoplasmic exosome function (*ski2*Δ) suggest decapping antagonists contribute to stress responses accompanying enhanced cell death (Fig. 7a and b).

Poly(A) tail length influences Pab1p binding, mRNA stability and translation in budding yeast (Beilharz and Preiss 2007; Meijer and de Moor 2011). Changes in poly(A) tail length of both cytoplasmic as well as nuclear mRNAs are now implicated in a number of physiological and pathological processes in higher eukaryotes (Weill *et al.*, 2012). Further studies are required to draw a correlation between poly(A) tail length control and apoptotic phenotype observed in yeast strains defective in decapping, cytoplasmic exosome function or deadenylation.

ACKNOWLEDGEMENTS

The authors acknowledge DBT-OU-ISLARE for providing instrumentation facility for flow cytometer and central facilities for research and development (CFRD), Osmania University, for confocal microscopy. The authors thank Dr Roy Parker, University of Colorado at Boulder for providing yeast strains yRP1195, yRP1616, yRP1619, yRP1620 and Dr Tharun Sundaresan, Uniformed Services University of the Health Sciences (USUHS), Bethesda for providing yeast strains yRP840, yRP1365 and yST456.

FUNDING

This research work was supported by science and engineering research board (SERB) and university grants commission (UGC), New Delhi, India.

Conflict of interest statement. None declared.

REFERENCES

Ahn SH, Diaz RL, Grunstein M, *et al.* Histone H2B deacetylation at lysine 11 is required for yeast apoptosis induced by phosphorylation of H2B at serine 10. *Mol Cell* 2006;**24**:211–20.

Amrani N, Ghosh S, Mangus DA, *et al.* Translation factors promote the formation of two states of the closed-loop mRNP. *Nature* 2008;**453**:1276–80.

Anderson JS, Parker RP. The 3′ to 5′ degradation of yeast mRNAs is a general mechanism for mRNA turnover that requires the SKI2 DEVH box protein and 3′ to 5′ exonucleases of the exosome complex. *EMBO J* 1998;**17**:1497–506.

Araki Y, Takahashi S, Kobayashi T, *et al.* Ski7p G protein interacts with the exosome and the Ski complex for 3′-to-5′ mRNA decay in yeast. *EMBO J* 2001;**20**:4684–93.

Beilharz TH, Preiss T. Widespread use of poly(A) tail length control to accentuate expression of the yeast transcriptome. *RNA* 2007;**13**:982–97.

Bouveret E, Rigaut G, Shevchenko A, *et al.* A Sm-like protein complex that participates in mRNA degradation. *EMBO J* 2000;**19**:1661–71.

Braun RJ, Zischka H. Mechanisms of Cdc48/VCP-mediated cell death: from yeast apoptosis to human disease. *Biochim Biophys Acta* 2008;**1783**:1418–35.

Brown CE, Sachs AB. Poly(A) tail length control in *Saccharomyces cerevisiae* occurs by message-specific deadenylation. *Mol Cell Biol* 1998;**18**:6548–59.

Carmona-Gutierrez D, Eisenberg T, Buttner S, *et al.* Apoptosis in yeast: triggers, pathways, subroutines. *Cell Death Differ* 2010;**17**:763–73.

Carmona-Gutierrez D, Madeo F. Tracing the roots of death: apoptosis in *Saccharomyces cerevisiae*. In: Dong Z, Yin X-M (eds). *Essentials of Apoptosis—A Guide for Basic and Clinical Research*. New York: Humana Press, 2009, 325–354.

Coller JM, Gray NK, Wickens MP. mRNA stabilization by poly(A) binding protein is independent of poly(A) and requires translation. *Gene Dev* 1998;**12**:3226–35.

Cooper M, Johnston LH, Beggs JD. Identification and characterization of Uss1p (Sdb23p): a novel U6 snRNA-associated protein with significant similarity to core proteins of small nuclear ribonucleoproteins. *EMBO J* 1995;**14**:2066–75.

Decker CJ, Parker R. A turnover pathway for both stable and unstable mRNAs in yeast: evidence for a requirement for deadenylation. *Gene Dev* 1993;**7**:1632–43.

Dunckley T, Parker R. The DCP2 protein is required for mRNA decapping in *Saccharomyces cerevisiae* and contains a functional MutT motif. *EMBO J* 1999;**18**:5411–22.

Fahrenkrog B, Sauder U, Aebi U. The *S. cerevisiae* HtrA-like protein Nma111p is a nuclear serine protease that mediates yeast apoptosis. *J Cell Sci* 2004;**117**:115–26.

Franks TM, Lykke-Andersen J. The control of mRNA decapping and P-body formation. *Mol Cell* 2008;**32**:605–15.

Funakoshi Y, Doi Y, Hosoda N, *et al.* Mechanism of mRNA deadenylation: evidence for a molecular interplay between translation termination factor eRF3 and mRNA deadenylases. *Genes Dev* 2007;**21**:3135–48.

Gasch AP, Spellman PT, Kao CM, *et al.* Genomic expression programs in the response of yeast cells to environmental changes. *Mol Biol Cell* 2000;**11**:4241–57.

Herker E, Jungwirth H, Lehmann KA, *et al.* Chronological aging leads to apoptosis in yeast. *J Cell Biol* 2004;**164**:501–7.

Higgins VJ, Alic N, Thorpe GW, *et al.* Phenotypic analysis of gene deletant strains for sensitivity to oxidative stress. *Yeast* 2002;**19**:203–14.

Ludovico P, Rodrigues F, Almeida A, *et al.* Cytochrome c release and mitochondria involvement in programmed cell death induced by acetic acid in *Saccharomyces cerevisiae*. *Mol Biol Cell* 2002;**13**:2598–606.

Madeo F, Frohlich E, Frohlich KU. A yeast mutant showing diagnostic markers of early and late apoptosis. *J Cell Biol* 1997;**139**:729–34.

Madeo F, Frohlich E, Ligr M, *et al*. Oxygen stress: a regulator of apoptosis in yeast. *J Cell Biol* 1999;**145**:757–67.

Madeo F, Herker E, Maldener IC, *et al*. Caspase-related protease regulates apoptosis in yeast. *Mol Cell* 2002;**9**:911–7.

Mazzoni C, D'Addario I, Falcone C. The C-terminus of the yeast Lsm4p is required for the association to P-bodies. *FEBS Lett* 2007;**581**:4836–40.

Mazzoni C, Falcone C. Isolation and study of KlLSM4, a Kluyveromyces lactis gene homologous to the essential gene LSM4 of Saccharomyces cerevisiae. *Yeast* 2001;**18**:1249–56.

Mazzoni C, Falcone C. Caspase-dependent apoptosis in yeast. *Biochim Biophys Acta* 2008;**1783**:1320–7.

Mazzoni C, Herker E, Palermo V, *et al*. Yeast caspase 1 links messenger RNA stability to apoptosis in yeast. *EMBO Rep* 2005;**6**:1076–81.

Mazzoni C, Mancini P, Madeo F, *et al*. A Kluyveromyces lactis mutant in the essential gene KlLSM4 shows phenotypic markers of apoptosis. *FEMS Yeast Res* 2003a;**4**:29–35.

Mazzoni C, Mancini P, Verdone L, *et al*. A truncated form of KlLsm4p and the absence of factors involved in mRNA decapping trigger apoptosis in yeast. *Mol Biol Cell* 2003b;**14**:721–9.

Meaux S, VanHoof A. Yeast transcripts cleaved by an internal ribozyme provide new insight into the role of the cap and poly(A) tail in translation and mRNA decay. *RNA* 2006;**12**:1323–37.

Meijer HA, de Moor CH. Fractionation of mRNA based on the length of the poly(A) tail. *Methods Mol Biol* 2011;**703**:123–35.

Muhlrad D, Decker CJ, Parker R. Deadenylation of the unstable mRNA encoded by the yeast MFA2 gene leads to decapping followed by 5′–>3′ digestion of the transcript. *Gene Dev* 1994;**8**:855–66.

Parker R, Song H. The enzymes and control of eukaryotic mRNA turnover. *Nat Struct Mol Biol* 2004;**11**:121–7.

Schwartz DC, Parker R. Mutations in translation initiation factors lead to increased rates of deadenylation and decapping of mRNAs in *Saccharomyces cerevisiae*. *Mol Cell Biol* 1999;**19**:5247–56.

Schwartz DC, Parker R. mRNA decapping in yeast requires dissociation of the cap binding protein, eukaryotic translation initiation factor 4E. *Mol Cel Biol* 2000;**20**:7933–42.

Sheth U, Parker R. Decapping and decay of messenger RNA occur in cytoplasmic processing bodies. *Science* 2003;**300**:805–8.

Steiger M, Carr-Schmid A, Schwartz DC, *et al*. Analysis of recombinant yeast decapping enzyme. *RNA* 2003;**9**:231–8.

Steller H. Mechanisms and genes of cellular suicide. *Science* 1995;**267**:1445–9.

Stevens A. 59-Exoribonuclease 1: Xrn1. *Method Enzymol* 2001;**342**:251–9.

Streicher KL, Yang ZQ, Draghici S, *et al*. Transforming function of the LSM1 oncogene in human breast cancers with the 8p11-12 amplicon. *Oncogene* 2007;**26**:2104–14.

Tarun SZ, Sachs AB. Association of the yeast poly(A) tail binding protein with translation initiation factor eIF-4G. *EMBO J* 1996;**15**:7168–77.

Teixeira D, Sheth U, Valencia-Sanchez MA, *et al*. Processing bodies require RNA for assembly and contain nontranslating mRNAs. *RNA* 2005;**11**:371–82.

Tharun S, He W, Mayes AE, *et al*. Yeast Sm-like proteins function in mRNA decapping and decay. *Nature* 2000;**404**:515–8.

Tharun S, Parker R. Targeting an mRNA for decapping: displacement of translation factors and association of the Lsm1p-7p complex on deadenylated yeast mRNAs. *Mol Cell* 2001;**8**:1075–83.

Thorpe GW, Fong CS, Alic N, *et al*. Cells have distinct mechanisms to maintain protection against different reactive oxygen species: oxidative-stress-response genes. *P Natl Acad Sci USA* 2004;**101**:6564–9.

Tucker M, Valencia-Sanchez MA, Staples RR, *et al*. The transcription factor associated Ccr4 and Caf1 proteins are components of the major cytoplasmic mRNA deadenylase in *Saccharomyces cerevisiae*. *Cell* 2001;**104**:377–86.

Van Dijk E, Cougot N, Meyer S, *et al*. Human Dcp2: a catalytically active mRNA decapping enzyme located in specific cytoplasmic structures. *EMBO J* 2002;**21**:6915–24.

Van Hoof A, Staples RR, Baker RE, *et al*. Function of the ski4p (Csl4p) and Ski7p proteins in 3′-to-5′ degradation of mRNA. *Mol Cell Biol* 2000;**21**:8230–43.

Walter D, Wissing S, Madeo F, *et al*. The inhibitor-of-apoptosis protein Bir1p protects against apoptosis in S. cerevisiae and is a substrate for the yeast homologue of Omi/HtrA2. *J Cell Sci* 2006;**119**:1843–51.

Weill L, Belloc E, Bava FA, *et al*. Translational control by changes in poly(A) tail length: recycling mRNAs. *Nat Struct Mol Biol* 2012;**19**:577–85.

Wells SE, Hillner PE, Vale RD, *et al*. Circularization of mRNA by eukaryotic translation initiation factors. *Mol Cell* 1998;**2**:135–40.

Wissing S, Ludovico P, Herker E, *et al*. An AIF orthologue regulates apoptosis in yeast. *J Cell Biol* 2004;**166**:969–74.

Yoon JH, Choi EJ, Parker R. Dcp2 phosphorylation by Ste20 modulates stress granule assembly and mRNA decay in *Saccharomyces cerevisiae*. *J Cell Biol* 2010;**189**:813–27.